nature biotechnology

LETTERS

https://doi.org/10.1038/s41587-019-0254-4

Adenine base editors catalyze cytosine conversions in human cells

Heon Seok Kim[1,2,3,7,8], You Kyeong Jeong[1,2,8], Junho K Hur[4,5], Jin-Soo Kim[3,6*] and Sangsu Bae[1,2*]

Adenine base editors comprise an adenosine deaminase, evolved in vitro, and a Cas9 nickase. Here, we show that in addition to converting adenine to guanine, adenine base editors also convert cytosine to guanine or thymine in a narrow editing window (positions 5–7) and in a confined TC*N sequence context. Adenine base editor–induced cytosine substitutions occur independently of adenosine conversions with an efficiency of up to 11.2% and reduce the number of suitable targeting sites for high-specificity base editing.

Base editing systems, including cytosine base editors (CBEs) and adenine base editors (ABEs), efficiently enable base substitutions without DNA cleavage or a requirement for template donor DNA[1–3]. The Liu group developed CBEs by combining APOBEC1 enzymes, which remove an amine group from cytosine, with catalytically dead Cas9 (dCas9) or Cas9 nickase (nCas9)[1] and ABEs by fusing an adenine deaminase to the Cas9 variants. Because an adenine deaminase that accepts single-stranded DNA as a substrate is unknown in nature, the authors created ssDNA-targetable enzymes by evolving an *Escherichia coli* adenine deaminase, TadA, targeting transfer RNAs (tRNAs). By introducing a number of mutations, Liu's group successfully constructed several versions of engineered TadAs (TadA*s) that target adenine in ssDNAs[3]. However, recently, Liu et al.[4] and Lee et al.[5] reported their observations of unexpected ABE-induced cytosine conversions in mouse embryos, but these conversions were thought to be exceptional and the characteristics of the engineered TadA* enzyme, including its target motifs inside the ssDNA, remain unknown.

To investigate whether ABEs are responsible for base conversions other than adenine substitutions, we carefully chose 22 human endogenous DNA target sites at which Cas9 nuclease activities are known to be sufficiently high (Supplementary Fig. 1)[6], to examine minor noncanonical base conversion effects of ABEs (Fig. 1a). We transfected plasmids expressing ABE v.7.10 (ABE7.10) and each single-guide RNA (sgRNA) into human embryonic kidney 293T (HEK293T) cells, and after 3 d we carefully inspected all base editing events caused by ABE7.10 at each nucleotide inside in the sgRNA binding regions by targeted deep sequencing and BE-analyzer software[7]. As expected, adenines in the editing windows were converted at high rates, with an average frequency of 40%. However, for two target sites in the *FANCF* and *RNF2* genes, noncanonical base editing of cytosine was also induced (Fig. 1b and Supplementary Fig. 2). The deep sequencing data showed that 10.9 and 10.2% of cytosines in the *FANCF* and *RNF2* target sites, respectively, were converted to other nucleotides by ABE7.10 (Fig. 1c and Supplementary Fig. 3).

We further examined whether these noncanonical cytosine conversion events varied depending on the ABE version used; these versions possess different mutations in the TadA enzyme. We repeated the experiments with ABE versions 6.3, 7.8 and 7.9 in addition to 7.10. Similarly to ABE7.10, ABE6.3, 7.8 and 7.9 also caused noncanonical editing events at cytosines in the two target sites (Fig. 1d). It is noteworthy that ABE7.8 and 7.9 induced cytosine conversions less frequently than ABE6.3 and 7.10, possibly indicating that the various TadA mutations affect the base editing specificity differently.

We next sought to examine the cause of ABE-induced cytosine conversions. We recognized that cytosine was converted to various nucleotides such as guanine and thymine via the action of ABEs, whereas adenine was dominantly converted to guanine, as shown at the substitution tables in Fig. 1c. The previous study reported that cytosine deamination by CBEs converted cytosine to guanine as well as thymine in the absence of uracil glycosylase inhibitor (UGI), but that cytosine was primarily converted to thymine in the presence of UGI[1,8]. Therefore, we hypothesized that the TadA* enzyme in ABEs deaminates not only the adenine but also the cytosine. To prove our hypothesis, we overexpressed UGI, which inhibits the excision of uracil and induces C-to-T substitutions[1,8], together with ABE7.10. We found that most cytosines were converted to thymine in the presence of excessive UGI, supporting our hypothesis that ABEs also directly deaminate cytosine (Fig. 1e and Supplementary Fig. 4).

We next investigated whether ABEs need specific DNA motifs for cytosine deamination. To investigate the effect of the nucleotide immediately adjacent to the cytosine, we chose 28 endogenous target sites with NC* sequences positioned in the center of the ABE7.10 editing window (that is, position 6), using Cas-OFFinder[9]. Among the tested NC* sequences, we observed that cytosines positioned just 3′ of a thymine were efficiently edited by ABE7.10, in sharp contrast to cytosines downstream of other nucleotides (Fig. 2a). Additionally, we examined the effect of nucleotides just 3′ of the cytosine after fixing the upstream nucleotide as thymine. We further chose 23 endogenous target sites with similar criteria as described above. In the TC*N sequences that we tested, we found that cytosines just 5′ of a pyrimidine were edited more efficiently, but that most cases underwent conversion at measurable levels regardless of the 3′ neighbor (Fig. 2b). From these observations, we conclude that the DNA target motif for cytosine deamination via ABEs is TC*N, which was confirmed by a computational de novo motif analysis (Fig. 2c).

We further investigated whether cytosine base editing via ABEs was affected by nearby adenine deamination events. To address this issue, we used two endogenous target sites that contained a TC*N

[1]Department of Chemistry, Hanyang University, Seoul, South Korea. [2]Research Institute for Natural Sciences, Hanyang University, Seoul, South Korea. [3]Center for Genome Engineering, Institute for Basic Science, Seoul, South Korea. [4]Department of Pathology, College of Medicine, Kyung Hee University, Seoul, South Korea. [5]Department of Biomedical Science, Graduate School, Kyung Hee University, Seoul, South Korea. [6]Department of Chemistry, Seoul National University, Seoul, South Korea. [7]Present address: Division of Oncology, Department of Medicine, Stanford University School of Medicine, Stanford, CA, USA. [8]These authors contributed equally: Heon Seok Kim, You Kyeong Jeong. *e-mail: jskim01@snu.ac.kr; sangsubae@hanyang.ac.kr

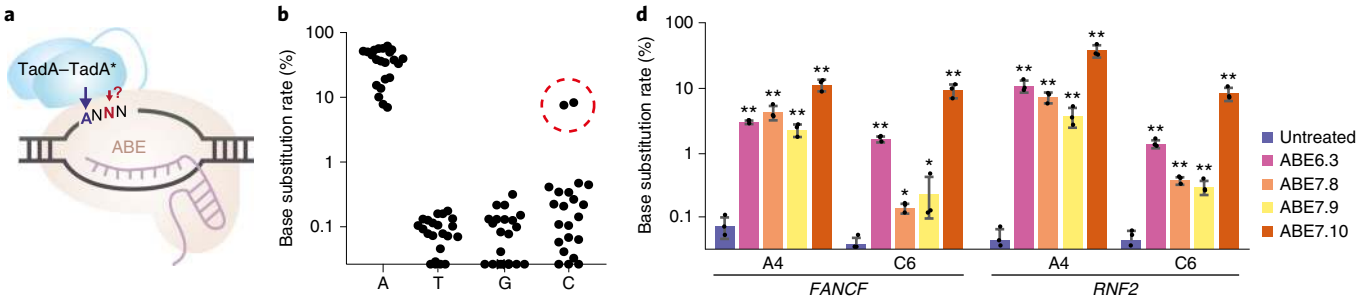

c

ABE7.10

FANCF	G	G	A	A4	T	C6	C	C	T	T	C	T	G	C	A	G	C	A	C	C	T	G	G
A	0	0	99.3	87.4	0	0.8	0.1	0.1	0.1	0	0	0	0	0.1	100	0.1	0.1	100	0.1	0.1	0.1	0	0.1
T	0	0	0	0	100	1.6	0	0.1	99.9	100	0	100	0	0.1	0	0	0	0	0	0	99.8	0	0
G	99.9	100	0.7	12.6	0	8.5	0	0	0	0	0	0	100	0	0	99.9	0	0	0	0	0.1	99.9	99.9
C	0	0	0	0.1	0	89.1	99.9	99.8	0	0	100	0	0	99.9	0	0	99.9	0	99.9	99.9	0.1	0	0

RNF2	G	T	C	A4	T	C6	T	T	A	G	T	C	A	T	T	A	C	C	T	G	A	G	G
A	0.1	0.1	0	56.7	0	0.1	0	0	91.0	0	0	0.1	99.9	0	0	99.9	0.1	0.1	0.1	0	99.9	0	0
T	0	99.9	0.1	0	99.9	1.4	99.9	99.9	0	0	99.9	0.1	0	99.9	99.9	0	0	0	99.8	0	0	0	0
G	99.9	0	0	43.2	0	8.6	0	0	8.9	99.9	0	0	0.1	0	0	0	0	0	0	99.9	0.1	99.9	99.9
C	0	0	99.8	0	0	89.8	0	0	0.1	0	0	99.8	0	0	0	0	99.9	99.8	0.1	0	0	0	0

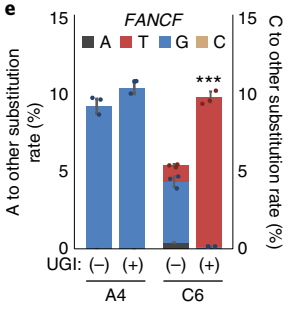

Fig. 1 | Cytosine editing by ABEs. a, Schematic diagram of ABE base editing specificities. **b**, Quantification of the substitution rate of each type of base in the ABE editing windows of a set of analyzed target sequences. **c**, Sequence tables showing nucleotide frequencies at each position in the targeted sites in two genes (*FANCF*, *RNF2*). Frequencies of expected nucleotides are highlighted in blue; frequencies of substituted nucleotides are highlighted in orange. PAM (protospacer adjacent motif) sequences are indicated in red. **d**, Analysis of base substitution efficiencies induced by various versions of ABE at A4 and C6 in the *FANCF* and *RNF2* sites. $^{*}P < 0.1$, $^{**}P < 0.001$. ($P = 0.0001$, 0.0010, 0.0006, 0.0004, 0.0001, 0.0010, 0.0995, 0.0008, 0.0003, 0.0031, 0.0005, 0.0005, 0.0002, 0.0016, 0.0007, 0.0001: Student's *t*-test, two-sided) ($n = 3$, mean ± s.d.) **e**, Effect of UGI on base editing at the *FANCF* site. The cytosine substitution rate was determined ($n = 3$, mean ± s.d.) $^{***}P = 0.00038$ (Student's *t*-test, two-sided). The proportion of edited base products from cytosine was also determined ($P = 0.000091$ (G), $P = 0.000005$ (T)).

motif positioned in the target window but that lacked adenine entirely. We found that cytosine was edited by ABE7.10 as usual in the absence of a neighboring adenine (Supplementary Fig. 5), indicating that cytosine deamination via ABEs is not a side effect induced after adenine deamination, but an independent event.

We further assumed that the preferred target window for cytosine deamination via ABEs might be different from the well-defined target window for adenine deamination. To determine the target window for efficient cytosine deamination, we chose a total of 29 endogenous target sites containing a TC*N motif at various positions in the region spanning nucleotides 4–9 inside the sgRNA binding region. We observed that cytosine editing via ABEs occurs at a maximum frequency at position 6 and that the editing window (that is, positions 5–7) is narrower compared to that of CBEs and the conventional adenine editing window of ABEs (Fig. 2d)[1,3]. We compared the cytosine conversion activities of ABEs to the activities of conventional CBEs at an identical target site and found that the CBEs showed higher cytosine editing efficiencies overall, but that the ABEs showed more specific cytosine conversions in narrower windows (Fig. 2e).

We further investigated whether the unexpected cytosine conversions induced by ABEs occur similarly in cancer- and noncancer-derived human cells. To address this issue, we repeated the above experiments using a more optimized version of ABE7.10, named ABEmax[10]. The results showed that cytosine base editing occurs at comparable levels for all tested cell lines (Fig. 2f and Supplementary Figs. 6–10). Furthermore, to confirm that ABE itself displays cytosine deaminase activity and to exclude any unknown possibilities that might lead to such activity in cells, we performed an in vitro ABE activity assay using purified ABE protein with sgRNAs. We then measured the resulting cytosine substitutions with targeted deep sequencing, directly verifying that ABE exhibits cytosine deaminase activity (Supplementary Fig. 11).

The ABE cytosine deamination activity is relatively minor compared to the canonical ABE adenine deamination activity (Supplementary Fig. 12), but is obviously independent. These results indicate that ABEs might be used for precise cytosine base editing in some specific cases, such as TCC-to-TGC or TCC-to-TTC conversions. On the other hand, it is reported that members of the APOBEC enzyme family, including rat APOBEC1 and human APOBECs share a consensus amino acid motif, (C/H)XEXnPCXXC[11], and have common preference for TC* motif in target DNA[1,12]. Because the engineered TadA* also has the motif in the core of the active site (Supplementary Fig. 13), we postulate that it has gained this unexpected cytosine deamination activity as well as a preference for target DNA sequences such as TC*N during the protein evolution process.

CRISPR-based base editing technologies, including CBEs and ABEs, have undoubtedly advanced the genome editing field. The advantage of BEs over the Cas9 nuclease has become more apparent after a recent study showing that CRISPR nuclease-mediated DNA cleavage at target sites frequently causes large deletions or genomic rearrangements[13]. However, it is notable that BEs induce off-target single-nucleotide conversions on DNA or RNA in the presence or absence of sgRNAs[14–20]. Our results raise another concern that ABEs can display unexpected on-target cytosine deamination activity.

Online content

Any methods, additional references, Nature Research reporting summaries, source data, statements of code and data availability and associated accession codes are available at https://doi.org/10.1038/s41587-019-0254-4.

Received: 4 March 2019; Accepted: 8 August 2019;
Published online: 23 September 2019

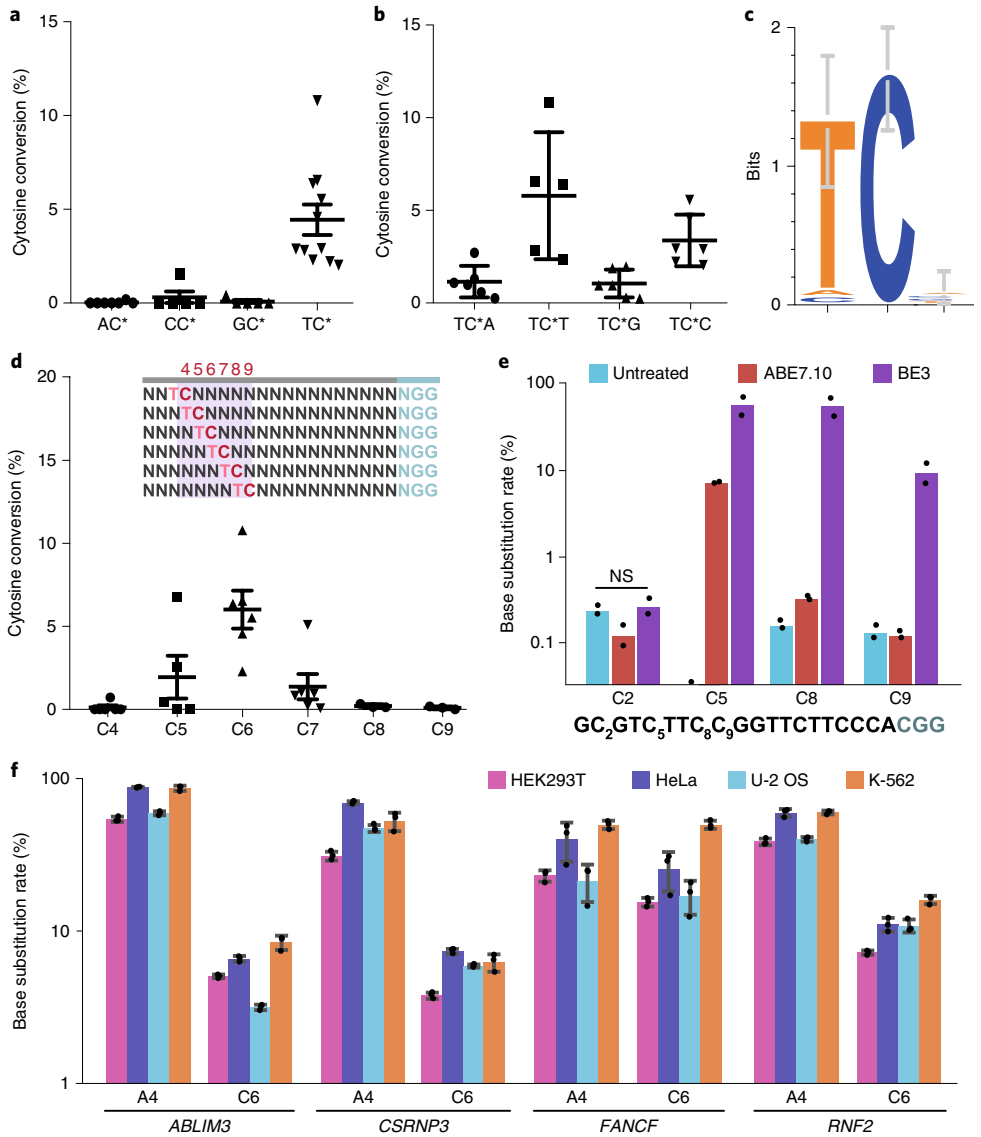

Fig. 2 | Sequence motif and editing window in cytosine editing by ABE7.10. a, Dependence of the cytosine (C*) substitution rate on the neighboring upstream base ($n=3$, mean ± s.d.). **b**, Dependence of the cytosine (C*) substitution rate on the neighboring downstream base ($n=3$, mean ± s.d.). **c**, DNA WebLogo created with target sequences in which cytosine editing was induced ($n=3$, mean ± s.d.). **d**, Cytosine substitution rate depending on the cytosine position in the editing window ($n=3$, mean ± s.d.). **e**, Comparison of BE3 and ABE7.10 cytosine editing windows in the *BIRC7* site ($n=2$, mean). NS, not significant. **f**, Cytosine editing efficiency of ABEmax in various cell lines ($n=3$, mean ± s.d.).

References

1. Komor, A. C., Kim, Y. B., Packer, M. S., Zuris, J. A. & Liu, D. R. Programmable editing of a target base in genomic DNA without double-stranded DNA cleavage. *Nature* **533**, 420–424 (2016).
2. Nishida, K. et al. Targeted nucleotide editing using hybrid prokaryotic and vertebrate adaptive immune systems. *Science* **353**, aaf8729 (2016).
3. Gaudelli, N. M. et al. Programmable base editing of A•T to G•C in genomic DNA without DNA cleavage. *Nature* **551**, 464–471 (2017).
4. Liu, Z. et al. Efficient generation of mouse models of human diseases via ABE- and BE-mediated base editing. *Nat. Commun.* **9**, 2338 (2018).
5. Lee, H. K. et al. Targeting fidelity of adenine and cytosine base editors in mouse embryos. *Nat. Commun.* **9**, 4804 (2018).
6. Park, J., Lim, K., Kim, J.-S. & Bae, S. Cas-analyzer: an online tool for assessing genome editing results using NGS data. *Bioinformatics* **33**, 286–288 (2017).
7. Hwang, G.-H. et al. Web-based design and analysis tools for CRISPR base editing. *BMC Bioinforma.* **19**, 542 (2018).
8. Ma, Y. et al. Targeted AID-mediated mutagenesis (TAM) enables efficient genomic diversification in mammalian cells. *Nat. Methods* **13**, 1029–1035 (2016).
9. Bae, S., Park, J. & Kim, J.-S. Cas-OFFinder: a fast and versatile algorithm that searches for potential off-target sites of Cas9 RNA-guided endonucleases. *Bioinformatics* **30**, 1473–1475 (2014).
10. Koblan, L. W. et al. Improving cytidine and adenine base editors by expression optimization and ancestral reconstruction. *Nat. Biotechnol.* **36**, 843–846 (2018).
11. Kuratani, M. et al. Crystal structure of tRNA adenosine deaminase (TadA) from *Aquifex aeolicus*. *J. Biol. Chem.* **280**, 16002–16008 (2005).
12. Wang, X. et al. Efficient base editing in methylated regions with a human APOBEC3A-Cas9 fusion. *Nat. Biotechnol.* **36**, 946–949 (2018).
13. Kosicki, M., Tomberg, K. & Bradley, A. Repair of double-strand breaks induced by CRISPR-Cas9 leads to large deletions and complex rearrangements. *Nat. Biotechnol.* **36**, 765–771 (2018).
14. Kim, D. et al. Genome-wide target specificities of CRISPR RNA-guided programmable deaminases. *Nat. Biotechnol.* **35**, 475–480 (2017).
15. Liang, P. et al. Genome-wide profiling of adenine base editor specificity by EndoV-seq. *Nat. Commun.* **10**, 67 (2019).
16. Kim, D., Kim, D., Lee, G., Cho, S.-I. & Kim, J.-S. Genome-wide target specificity of CRISPR RNA-guided adenine base editors. *Nat. Biotechnol.* **37**, 430–435 (2019).

17. Jin, S. et al. Cytosine, but not adenine, base editors induce genome-wide off-target mutations in rice. *Science* **364**, 292–295 (2019).
18. Zuo, E. et al. Cytosine base editor generates substantial off-target single-nucleotide variants in mouse embryos. *Science* **364**, 289–292 (2019).
19. Grünewald, J. et al. Transcriptome-wide off-target RNA editing induced by CRISPR-guided DNA base editors. *Nature* **569**, 433–437 (2019).
20. Zhou, C. et al. Off-target RNA mutation induced by DNA base editing and its elimination by mutagenesis. *Nature* **571**, 275–278 (2019).

Acknowledgements

We thank G.-H. Hwang for his support on bioinformatics analysis; J.-S. Woo and S.-N. Lee for supplying purified ABE proteins. This research was supported by grants from IBS (no. IBS-R021-D1 to J.S.K.), the National Research Foundation of Korea (grant nos. 2017R1D1A1B03035094, 2017R1E1A1A01074529 and 2018M3A9H3021707 to J.K.H. and 2018M3A9H3022412 to S.B.) and the Next Generation BioGreen 21 Program (no. PJ01319301), Korea Healthcare Technology R&D Project (no. HI16C1012) and Technology Innovation Program (no. 20000158) to S.B.

Author contributions

H.S.K., J.S.K. and S.B. conceived this project. H.S.K. and Y.K.J. performed the experiments and bioinformatics analyses. J.K.H. gave critical comments. H.S.K. and S.B. wrote the manuscript with the approval of all other authors. J.S.K. and S.B. supervised the research.

Competing interests

S.B., J.-S.K., H.S.K. and Y.K.J. have filed a patent application based on this work.

Additional information

Supplementary information is available for this paper at https://doi.org/10.1038/s41587-019-0254-4.

Reprints and permissions information is available at www.nature.com/reprints.

Correspondence and requests for materials should be addressed to J.-S.K. or S.B.

Publisher's note Springer Nature remains neutral with regard to jurisdictional claims in published maps and institutional affiliations.

Methods

Cell culture conditions. HEK293T (ATCC CRL-11268), HeLa (ATCC CLL-2), U-2 OS (ATCC HTB-96) and K-562 (ATCC CCL-243) cells were maintained in DMEM supplemented with 10% FBS, 100 μg ml^{-1} streptomycin, 100 units per ml penicillin and 0.1 mM nonessential amino acids. GM14867 cells, human fibroblasts derived from a patient containing mutations in the xeroderma pigmentosum, complementation group C (XPC) gene, were purchased from the Coriell Institute. GM14867 cells were maintained in MEM supplemented with 15% FBS and a penicillin/streptomycin mix.

Transfection conditions. Here, 1.0×10^5 HEK293T cells were plated 1 d before transfection. The ABE expression plasmid (750 ng) and sgRNA plasmids (250 ng) were transfected into cells using Lipofectamine 2000 (Invitrogen) according to the manufacturer's protocol. To maintain parallel conditions, a 4D-nucleofector (Lonza) was used for HEK293T, HeLa, U-2 OS, K-562 and GM14867 cells. The ABEmax expression plasmid (750 ng) and sgRNA plasmids (250 ng) were electroporated into 2.0×10^5 cancer cells according to the manufacturer's protocol. In the case of GM14867 cells, ABEmax plasmid (14 μg) and sgRNA plasmid (6 μg) were electroporated into 8×10^5 fibroblasts as described before[21]. Appropriate nucleofector programs were used for each cell line (the CM-130 program for HEK293T, the CN-114 program for HeLa, the CM-104 program for U-2 OS, the FF-120 program for K-562 and the DS-137 program for GM14867). Genomic DNA was also isolated 72 h after transfection.

UGI overexpression. We constructed the CMV-UGI plasmid based on pCMV-BE3 (Addgene, no. 73021). To overexpress UGI together with ABE, the ABE expression plasmid (500 ng), sgRNA plasmids (250 ng) and pCMV-UGI (250 ng) were transfected using Lipofectamine 2000. For a negative control, we transfected the same amount of an empty pCMV vector instead of pCMV-UGI.

In vitro ABE activity assay. The in vitro deamination assay was performed as previously described[16]. Briefly, recombinant ABE protein (2,000 ng) and sgRNA (1,500 ng) were pre-incubated for 5 min at room temperature. Genomic DNA (500 ng) purified from HEK293T cells and 2× buffer were added to the ABE-sgRNA complexes; the final volume of 50 μl contained 50 mM Tris-HCl, 25 mM KCl, 2.5 mM $MgSO_4$, 10% glycerol, 2 mM DTT and 10 mM $ZnCl_2$. The mixture was incubated at 37 °C overnight. Products were purified using a genomic DNA prep kit (QIAGEN, catalog no. 69504) and amplified using PCR. Final PCR products were analyzed using targeted deep sequencing.

Targeted deep sequencing. On-target sites were amplified with a KAPA HiFi HotStart PCR kit (KAPA Biosystems no. KK2501) for sequencing library generation. These libraries were sequenced using MiniSeq with a TruSeq HT Dual Index system (Illumina) as described before[22]. Briefly, equal amounts of the PCR amplicons were subjected to paired-end read sequencing using Illumina MiniSeq platform. Samples were sequenced at a sequencing depth of average $30{,}067 \pm 1{,}290\times$ ($n = 137 \pm$ s.e.m.). Rare sequence reads <1 were excluded.

Statistics. Statistics were calculated using GraphPad Prism v.8 and OriginPro 2016. *P* values were calculated by a two-sided test.

Reporting Summary. Further information on research design is available in the Nature Research Reporting Summary linked to this article.

Data availability

High–throughput sequencing data have been deposited in the NCBI Sequence Read Archive database under accession number PRJNA525294.

References

21. Lee, C. et al. CRISPR-Pass: gene rescue of nonsense mutations using adenine base editors. *Mol. Ther.* **27**, 1364–1371 (2019).
22. Cho, S. W. et al. Analysis of off-target effects of CRISPR/Cas-derived RNA-guided endonucleases and nickases. *Genome Res.* **24**, 132–141 (2014).

nature research

Corresponding author(s): Sangsu Bae

Last updated by author(s): Aug 6, 2019

Reporting Summary

Nature Research wishes to improve the reproducibility of the work that we publish. This form provides structure for consistency and transparency in reporting. For further information on Nature Research policies, see Authors & Referees and the Editorial Policy Checklist.

Statistics

For all statistical analyses, confirm that the following items are present in the figure legend, table legend, main text, or Methods section.

n/a	Confirmed	
☐	☒	The exact sample size (*n*) for each experimental group/condition, given as a discrete number and unit of measurement
☐	☒	A statement on whether measurements were taken from distinct samples or whether the same sample was measured repeatedly
☐	☒	The statistical test(s) used AND whether they are one- or two-sided *Only common tests should be described solely by name; describe more complex techniques in the Methods section.*
☒	☐	A description of all covariates tested
☒	☐	A description of any assumptions or corrections, such as tests of normality and adjustment for multiple comparisons
☐	☒	A full description of the statistical parameters including central tendency (e.g. means) or other basic estimates (e.g. regression coefficient) AND variation (e.g. standard deviation) or associated estimates of uncertainty (e.g. confidence intervals)
☐	☒	For null hypothesis testing, the test statistic (e.g. *F*, *t*, *r*) with confidence intervals, effect sizes, degrees of freedom and *P* value noted *Give P values as exact values whenever suitable.*
☒	☐	For Bayesian analysis, information on the choice of priors and Markov chain Monte Carlo settings
☒	☐	For hierarchical and complex designs, identification of the appropriate level for tests and full reporting of outcomes
☒	☐	Estimates of effect sizes (e.g. Cohen's *d*, Pearson's *r*), indicating how they were calculated

Our web collection on statistics for biologists contains articles on many of the points above.

Software and code

Policy information about availability of computer code

Data collection	No softwares were used
Data analysis	Cas-OFFinder, Cas-Analyzer, BE-analyzer (http://www.rgenome.net/), Excel, Graph pad prism, Adobe illustrator, OriginPro 2016

For manuscripts utilizing custom algorithms or software that are central to the research but not yet described in published literature, software must be made available to editors/reviewers. We strongly encourage code deposition in a community repository (e.g. GitHub). See the Nature Research guidelines for submitting code & software for further information.

Data

Policy information about availability of data

All manuscripts must include a data availability statement. This statement should provide the following information, where applicable:

- Accession codes, unique identifiers, or web links for publicly available datasets
- A list of figures that have associated raw data
- A description of any restrictions on data availability

High–throughput sequencing data have been deposited in the NCBI Sequence Read Archive database (SRA; https://www.ncbi.nlm.nih.gov/sra) under accession number PRJNA525294.

Field-specific reporting

Please select the one below that is the best fit for your research. If you are not sure, read the appropriate sections before making your selection.

☒ Life sciences ☐ Behavioural & social sciences ☐ Ecological, evolutionary & environmental sciences

Life sciences study design

All studies must disclose on these points even when the disclosure is negative.

Sample size	No statistical methods were used to predetermine sample size for experiments.
Data exclusions	There are no excluded data.
Replication	The data we showed are replicated more than two times for cell line tests.
Randomization	Samples were not randomized.
Blinding	The investigators were not blinded to group allocation.

Reporting for specific materials, systems and methods

We require information from authors about some types of materials, experimental systems and methods used in many studies. Here, indicate whether each material, system or method listed is relevant to your study. If you are not sure if a list item applies to your research, read the appropriate section before selecting a response.

Materials & experimental systems

n/a	Involved in the study
☒	☐ Antibodies
☐	☒ Eukaryotic cell lines
☒	☐ Palaeontology
☒	☐ Animals and other organisms
☒	☐ Human research participants
☒	☐ Clinical data

Methods

n/a	Involved in the study
☒	☐ ChIP-seq
☒	☐ Flow cytometry
☒	☐ MRI-based neuroimaging

Eukaryotic cell lines

Policy information about cell lines

Cell line source(s)	HEK293T, HeLa, K562, U2-OS were purchased from ATCC. GM14867 were from Coriell Institute.
Authentication	No cell lines were authenticated
Mycoplasma contamination	Cells were not tested for mycoplasma contamination.
Commonly misidentified lines (See ICLAC register)	Not mentioned